J Mater Sci (2008) 43:7397–7402
DOI 10.1007/s10853-008-2873-x

ULTRAFINE-GRAINED MATERIALS

Property optimization of nanostructured ARB-processed Al by post-process deformation

X. Huang · N. Kamikawa · N. Hansen

Received: 6 March 2008 / Accepted: 10 July 2008 / Published online: 7 August 2008

Abstract The effect of post-process deformation on the mechanical properties of nanostructured aluminum (99.2% purity) has been investigated by cold rolling of samples which have been processed by accumulative roll bonding (ARB) to a strain of $\varepsilon_{vM} = 4.8$. Samples have been cold rolled to 10, 15, and 50% reductions and ultimate tensile strength (UTS), yield stress and elongation have been determined by tensile testing at room temperature. The mechanical testing shows that cold rolling to low strains (10% and 15%) leads to softening and increase in elongation compared to the as-processed ARB material. In contrary, cold rolling to large strain (50%) results in significant strengthening. This leads to the suggestion of a transition strain within the range of 25–35% reduction by rolling. The microstructural evolution during post-process deformation has been followed by transmission electron microscopy showing a significant change in the dislocation structure when the strain is increased. Based on the experimental observations the mechanical behavior is related to the structural changes focusing on the characteristics of the dislocation structure present between the narrowly spaced lamellar boundaries in the deformed structure.

Introduction

It has been well established that nanostructured metals produced by high strain deformation is characterized by a mixture of high angle boundaries (often > 60%) and low angle dislocation boundaries [1–4]. Furthermore, the presence of a density of interior dislocations within the volumes between the boundaries is also a common feature although the density of these dislocations depends strongly on the metal and the processing procedure applied [5–9]. These structural features lead to characteristic strengthening mechanisms and mechanical behavior of nanostructured metals as compared to recrystallized metals. For example, both grain boundary strengthening related to the refined structure and dislocation strengthening must be considered to understand the high strength observed in the nanostructured metals [1, 7, 9–11]. Another characteristic is the relatively large post-necking elongation observed in nanostructured fcc metals, which may relate to the elevated strain rate sensitivity of the flow stress achieved by the fine structure and the presence of dislocations [12, 13].

The importance of dislocations present in the nanostructured metals in determining the mechanical behavior has been explored in our recent studies [12, 14, 15], showing that the presence of a low density of mobile dislocations can introduce softening rather than a hardening of the metal. Based on this finding, a new strategy to enhance the ductility of nanostructured metals by a slight post-process deformation has been proposed [14]. This new strategy has been explored in both nanostructured Al and interstitial free steel processed by accumulative roll bonding (ARB), and in both metals a beneficial effect on the tensile elongation was observed after 15% cold rolling [12].

To further explore this new strategy and understand the beneficial effect of post-process deformation, we have in this study applied different rolling reductions to a recovery-annealed nanostructured Al produced by ARB. The mechanical behavior is evaluated by tensile testing and related to the structural evolution that is characterized by transmission electron microscopy.

X. Huang (✉) · N. Kamikawa · N. Hansen
Center for Fundamental Research: Metal Structures in Four Dimensions, Materials Research Department, Risø National Laboratory for Sustainable Energy, Technical University of Denmark, 4000 Roskilde, Denmark
e-mail: xiaoxu.huang@risoe.dk

Experimental

Commercial purity aluminum (99.2% pure) was used in this study, having a chemical composition which is given in Table 1. Fully recrystallized material with a mean grain size of 22 μm was produced by cold-rolling and annealing, and used as the starting material for ARB processing. After degreasing the surfaces by acetone and wire-brushing, two sheets of the starting material were stacked and roll-bonded to 50% reduction (corresponding to a true rolling strain of 0.69 or an equivalent strain of 0.8) in a single pass at room temperature. The roll-bonding was carried out by a two-high rolling mill with rolls of 310 mm diameter under dry conditions without using any lubricant. The roll-bonded sheets were immediately water-cooled after roll-bonding. The roll-bonded sheet was cut into half length and subjected to the next cycle of ARB processing. The procedure of cutting, stacking, and roll-bonding, referred to as one cycle of ARB, was repeated up to six cycles, accumulating an equivalent strain of 4.8. The rolling direction (RD) was unchanged during the processing. Note that the large rolling draught applied in each ARB cycle and the dry rolling condition introduced significant redundant shear at the sample surface, which increases the nominal strain and enhances the structural refinement during the processing [16].

The six-cycle ARB-processed samples were annealed at 150 °C for 30 min to reduce the density of dislocations present in the structure [14]. Several samples annealed under this condition were subjected to further cold rolling to different reductions to investigate the effect of post-process deformation on the mechanical behavior and microstructural evolution. The cold rolling was conducted in a two-high mill with 75 mm diameter rolls. Three different rolling reductions, 10, 15, and 50%, in thickness were imposed in a single pass, two passes, and five passes, respectively. These rolling schemes generated ratios between the contact length and the sample thickness in the range of 1.5–3.0, resulting in a homogeneous deformation during the cold rolling process. After each pass cold rolling the samples were water-cooled.

The above treatment produced five types of samples, as listed in Table 2, for mechanical and structural characterization. The mechanical properties of the specimens were evaluated by tensile testing at room temperature using an Instron testing machine. Tensile specimens had a gauge dimension of 10 mm long and 5 mm wide. The strain rate of tensile testing was on the order of 10^{-4} s^{-1}. The tensile strain was recorded using an extensometer.

Table 1 Chemical composition of a commercial purity Al (1100) (mass%)

Si	Fe	Cu	Mn	Mg	Ti	B	V	Ni	Al
0.11	0.55	0.11	0.01	0.02	0.02	0.0007	0.011	0.003	Bal.

Table 2 Treatment conditions to prepare samples for tensile test and microstructural analysis

Sample	Treatment
1	As-ARB (six cycles, strain = 4.8)
2	1 + 150 °C, 30 min
3	2 + 10% CR
4	2 + 15% CR
5	2 + 50% CR

The microstructural characterization was carried out mainly by transmission electron microscopy (TEM). TEM analyses were made in the longitudinal section, containing the normal direction (ND) and the RD of deformed sheets, as it is the best section to reveal the detailed structural features for cold rolled samples [17]. Thin TEM foils were prepared by electropolishing at −15 °C and at a voltage of 20 V in a 300 mL HNO_3 + 700 mL CH_3OH solution. The foils were examined with a JEOL 2000FX electron microscope operating at 200 kV. An online Kikuchi pattern analysis technique [18] was used for measurements of orientation and misorientation. The dislocation density was measured using the intercept method. The foil thickness was determined by means of convergent beam diffraction.

Mechanical behavior

Figure 1 shows the tensile stress–strain curves of the as-ARB sample and the low temperature annealed sample. It is seen that the as-ARB-processed sample (curve 1) shows an ultimate tensile strength of 322 MPa which is reached at a relatively low strain (1.6%) and a total elongation of

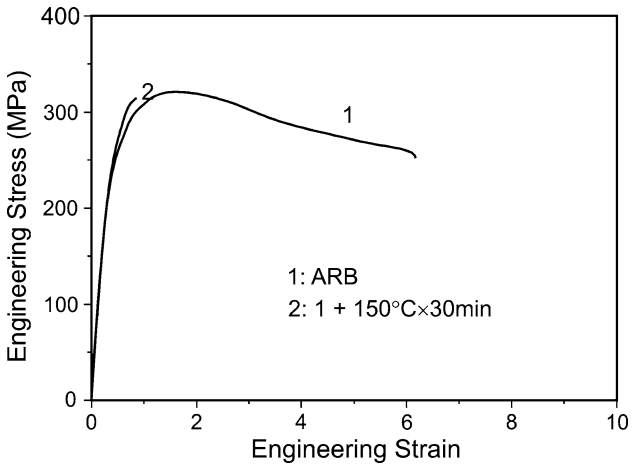

Fig. 1 Tensile stress–strain curves of a six-cycle ARB Aluminum sample (curve 1) and an annealed sample after the ARB processing to six cycles (curve 2). Refer to Table 2 for sample numbering

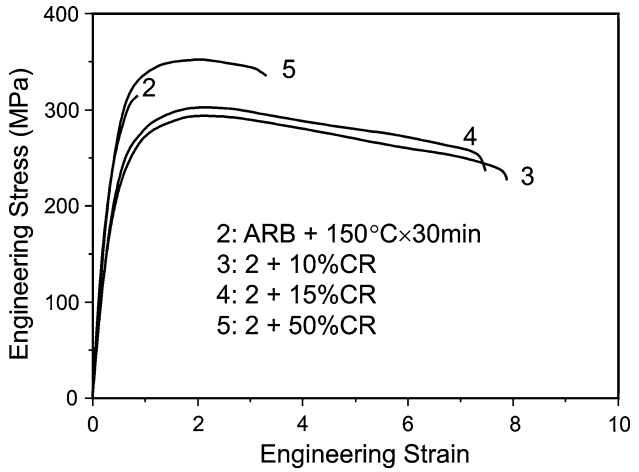

Fig. 2 Tensile stress–strain curves of three annealed ARB samples followed by cold rolling to 10, 15 and 50% thickness reduction. For comparison, the curve of the annealed sample is also included. Refer Table 2 for sample numbering

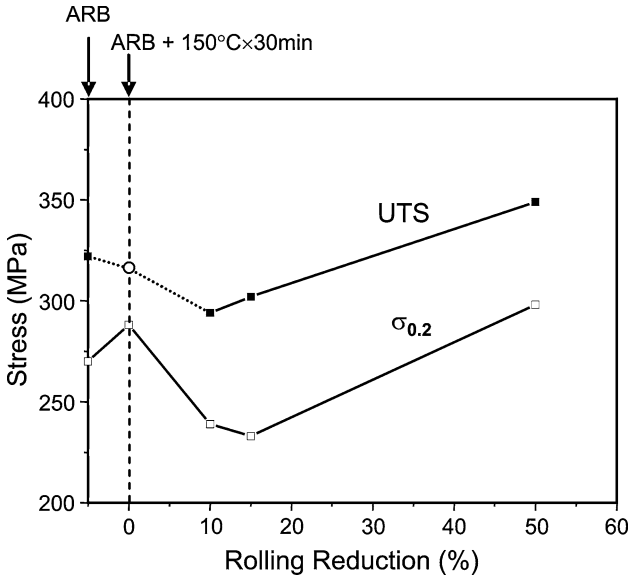

Fig. 3 Effect of cold rolling reduction on the strength of annealed ARB samples. Note that softening occurs at the low strain, followed by a hardening at the high strain

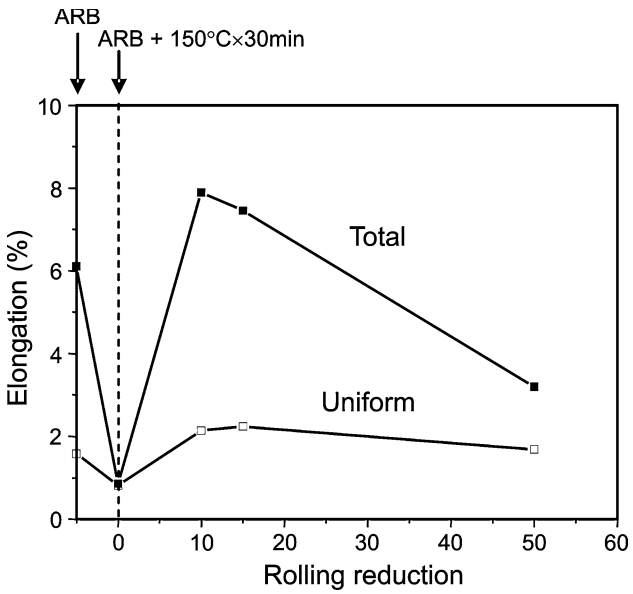

Fig. 4 Effect of cold rolling reduction on the uniform and total elongation of the annealed ARB samples. Note the significant enhancement in the elongation after low strain cold rolling

6.1% mostly being post-necking elongation. After annealing at 150 °C for 30 min (curve 2), the yield stress increased to 288 MPa (Fig. 2), but a premature failure occurred at a very low strain (0.8%), which is associated with a maximum stress of 316 MPa slightly lower than the UTS observed in the as-ARB sample. Note that these tensile stress strain curves are almost identical to those reported previously for samples that were processed under similar ARB conditions and annealing condition [14].

Figure 2 shows the stress–strain curves of annealed samples followed by cold rolling to 10, 15, and 50% reductions. It is seen that the deformation by 10 or 15% cold rolling causes a significant decrease in the strength and a significant enhancement in the elongation (curves 3 and 4) as compared with the annealed sample (curve 2). These results confirm the occurrence of softening by a low strain post-process deformation as reported previously [12, 14]. However, after 50% cold rolling (curve 5), the sample shows a stress level higher than all the other samples over the entire plastic strain range until the fracture occurs. This indicates that the large strain cold rolling has hardened rather than softened the sample. It is interesting to note that curve 5 is approximately parallel to the curves 3 and 4, indicating a similar stability of deformation in these cold rolled samples. One of the reasons for the lower elongation observed in sample 5 than in samples 3 and 4 might be the thinner sample thickness caused by the higher rolling reduction.

From these curves shown in Figs. 1 and 2, the yield stress at 0.2% plastic strain, the UTS (the maximum stress for the annealed sample, sample 2), the uniform elongation, and the total elongation were measured and plotted in Figs. 3 and 4. From Fig. 3, it is clearly seen that both the yield stress and the UTS of the 10 and 15% cold rolled samples are lower than the as-ARB sample. Figure 4 shows that both the uniform and the total elongation are better in these two samples than obtained in the as-ARB sample.

To summarize, it has been observed that the post-process deformation has a strong effect on the mechanical behavior, which is reflected in the occurrence of softening or hardening depending on the rolling reduction applied to

the annealed sample. This observation indicates that the mechanical behavior of nanostructured metals is quite sensitive to the structural condition which can be modified in a controllable way by the post-process annealing or deformation.

Structural evolution

The microstructures in the six-cycle ARB sample and the low temperature annealed sample have been well characterized previously [14]. Figure 5 illustrates typical examples of TEM observations for these two sample conditions. As shown in Fig. 5a, a well-developed lamellar structure of nanometer scale is seen, which is delineated by extended lamellar boundaries parallel to the rolling plane and short boundaries interconnecting the lamellar boundaries. The presence of individual dislocations or loose dislocation tangles is observed within the lamellae that are oriented in strong diffraction conditions (showing dark contrast). Sample tilting in the TEM confirmed that almost all lamellae contain dislocations and higher dislocation densities were often found in the lamellae that are relatively coarse. The structural parameters including spacing, misorientation angle, and density of interior dislocations have been quantified for these two samples. The key observations in the as-ARB samples were the bimodal distribution of misorientation angles, more than 60% high angle boundaries and an interior dislocation density as high as 1.3×10^{14} m^{-2}. After recovery annealing at 150 °C for 30 min, the main structural changes observed were (1) a decrease in the density of interior dislocations from 1.3×10^{14} m^{-2} in the deformed state to 0.5×10^{14} m^{-2} after annealing, (2) a decrease in the fraction of low angle boundaries (<2°) (from 13% to 10%) and (3) a slight structural coarsening associated with a decrease of the aspect ratio between the spacings of lamellar boundaries and interconnecting boundaries and with a sharpening of both types of boundaries.

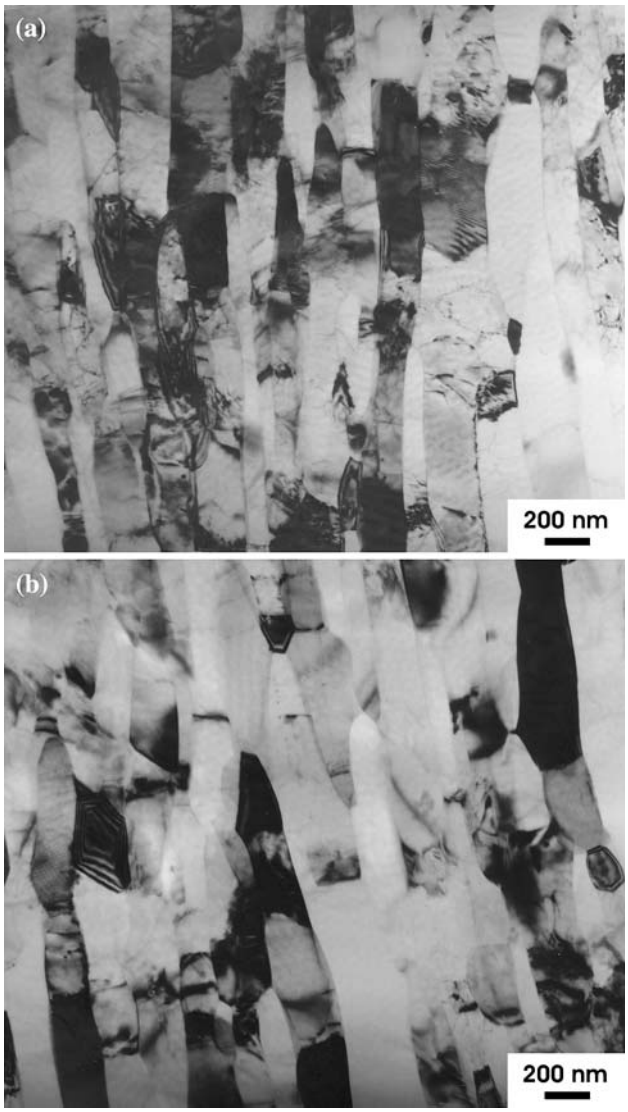

Fig. 5 TEM images showing the typical morphology of a lamellar structure developed in the six-cycle ARB-processed sample (**a**) and the structural changes after annealing at 150 °C for 30 min (**b**). Note the morphological change and the annihilation of interior dislocations after the annealing

Figure 6 shows TEM images of 15 and 50% cold rolled samples after annealing. Compared with the annealed sample (Fig. 5b), several structural changes were found based on morphological observations and structural parameter quantification. As seen in Fig. 6, dislocations are reintroduced into the lamellae with a high dislocation density often being seen in the coarser lamellae. In the 15% cold rolled sample, the introduced dislocations are mostly present as single dislocations and the extent of dislocation tangling is not significant. With an increase in the rolling reduction to 50%, dislocation tangles and network were often observed within the lamellae. The interconnecting boundaries become less clearly defined due to the presence of many dislocations. Figure 7 shows the quantification of the mean dislocation density for samples in different conditions. Clearly the dislocation density has been increased significantly after 50% cold rolling. Figure 8 shows the variation of lamellar boundary spacing against the rolling reduction. Interestingly, the lamellar boundary spacing is refined to 160 nm which is the smallest spacing ever obtained by cold rolling [2] or ARB [14] for commercial purity Al. This refinement in the lamellar boundary may be one of the causes to the significant increase in flow stress after 50% reduction.

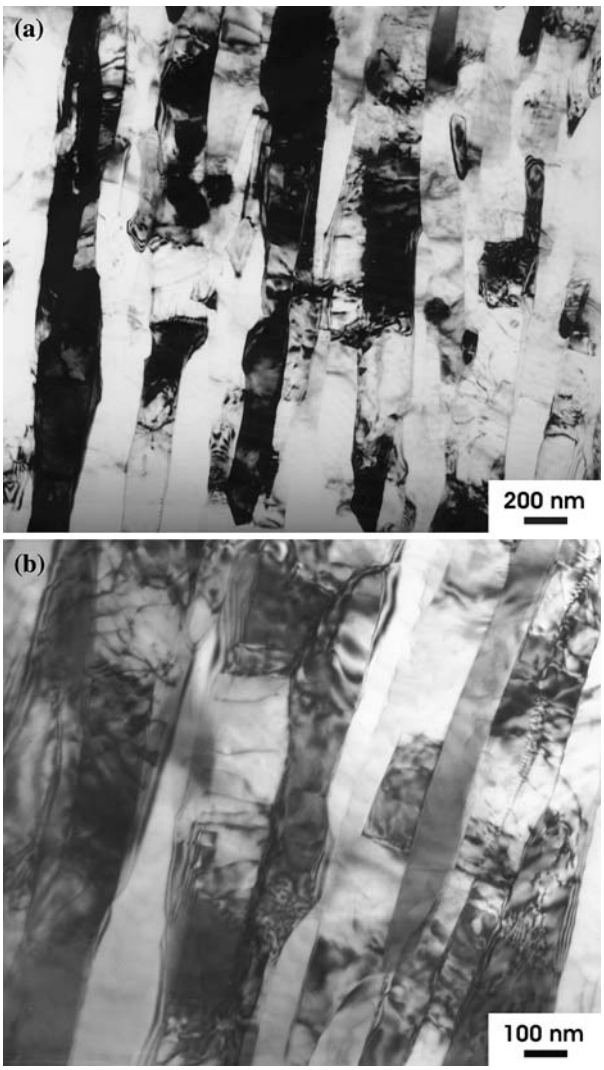

Fig. 6 TEM images showing the lamellar structure and the introduction of dislocations within the lamellae after 15% (**a**) and 50% (**b**) cold rolling of the samples annealed at 150 °C for 30 min

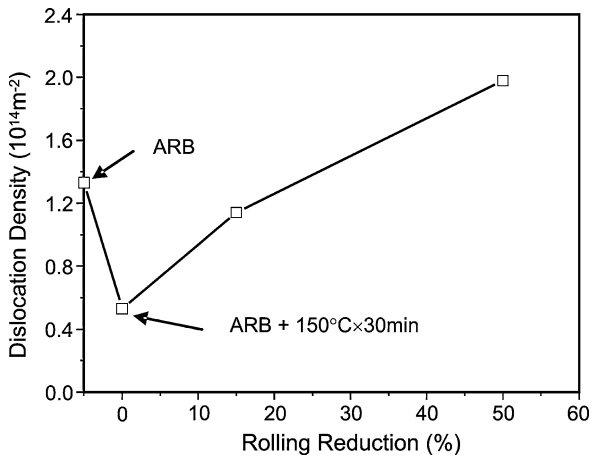

Fig. 7 Variation of mean dislocation density with the sample condition

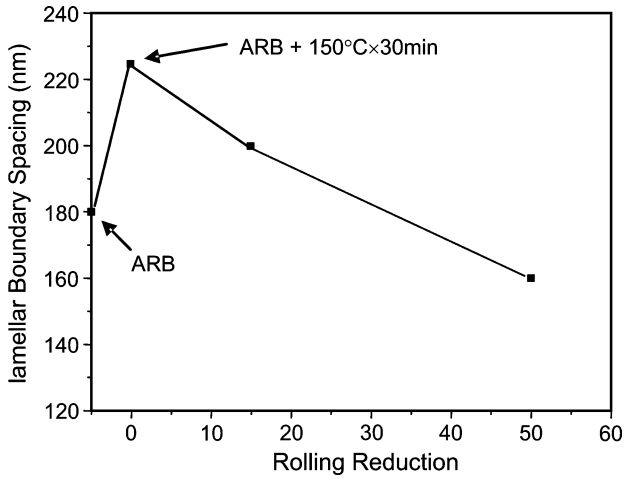

Fig. 8 Change of lamellar boundary spacing with the sample condition

Structure and property relation

The present results show that the effect of post-process deformation on the yield strength of nanostructured Al is not a monotonic function of the rolling reduction. As shown in Fig. 3, the yield strength decreases quickly with strain in the low strain range, followed by a gradual increase with further straining. In other words, a deformation-induced decrease in the yield strength (softening) in the nanostructured Al occurs only when the strain is lower than a certain value, and a deformation-induced increase in the yield strength (hardening) takes place again when the strain is above this value. The strain at which the transition from deformation-induced softening to hardening takes place may depend on the structural parameters such as the boundary spacing, the high angle boundary fraction, and the initial dislocation density. In this study, the effect of post-process deformation was examined for the initial structure produced by six-cycle ARB followed by a low temperature annealing (150 °C, 30 min). The structural parameters in this initial state are characterized by a nanoscale lamellar boundary spacing (225 nm), a high fraction of high angle boundaries (64%), and a low dislocation density (0.5×10^{14} m^{-2}). For such a nanostructured Al, the transition strain is identified to be in the range 25–35%, as seen in Fig. 3. This transition strain corresponds to a critical dislocation density of about 1.5×10^{14} m^{-2} (Fig. 7), which is higher than the dislocation density in the as-ARB sample. Therefore, a slight deformation of the as-ARB sample will cause a decrease in the yield strength, which was observed previously [14]. The transition strain may increase with decreasing the grain size or increasing the fraction of high angle boundaries, but may decrease with increasing the dislocation density in the initial nanostructure. If the initial dislocation density is too high, as in

highly deformed copper and nickel, the deformation-induced decrease in the yield strength may not occur.

This dependence of the occurrence of deformation-induced decrease or increase in the yield strength (softening or hardening) on the prost-process strain must relate to the internal change in the structural parameters. The introduction of mobile dislocations and dislocation sources by a slight cold rolling has been proposed to be the cause for the deformation-induced softening in nanostructured materials [14, 15]. This explains the observation of a rather significant decrease in the yield stress in the 10 and 15% deformed samples as loose dislocations are introduced in these samples (e.g. Fig. 6a). However, when a higher density of dislocations is introduced into the sample, they interact with each other forming strong tangles and network (Fig. 6b). As a result, both the density of the dislocations that is free to move when a stress is applied and the free length of dislocation segments that can act as dislocation sources decrease. Therefore, the softening effect by mobile dislocations and easy dislocation sources is reduced and a large portion of dislocations present in such a structure will contribute to a dislocation forest hardening, leading to a net increase in strength.

The present results further proved the strategy proposed in our previous study [14] that the ductility of nanostructured metals characterized by a high fraction of high angle boundaries can be enhanced by introducing a certain density of free dislocations in the nanostructured metals. For the nanostructured Al investigated in the present study, the dislocation density showing an optimized strength and ductility is of the order of 1–2 $\times$ 10^{14} m^{-2}. It is interesting to note that a similar strategy was proposed [9] for toughening the ultrafine grain Cu that was characterized by a grain size of 180 nm, a high angle boundary fraction of 56%, and an initial dislocation density of 2.3 $\times$ 10^{14} m^{-2}.

Conclusions

A nanostructured Al has been prepared by accumulative roll bonding and low temperature annealing. Further cold rolling has been applied to this material to investigate the effect of rolling reduction on the mechanical behavior and microstructural evolution.

(1) A softening characterized by a decrease in the yield stress is observed when the rolling reduction is low (10 and 15%), while a hardening occurs after 50% reduction by cold rolling. The transition from softening to hardening corresponds to 25–35% rolling reduction.

(2) Dislocations are introduced during the cold rolling and the interior dislocation density increases with the rolling reduction. However, there is a change in the dislocation configurations when the strain is increased from 15% to 50%. At the low strain, the interior dislocations are principally present as loose dislocations which are supposed to be free to move when a stress is applied. At the high strain, the dislocations form tangles and networks. This change in the characteristics of dislocation structure is considered to be the cause for the transition from softening to hardening.

(3) The lamellar spacing gradually decreases with increasing rolling reduction to 160 nm, enhancing the strength contribution from lamellar boundaries. The maximum stress obtained is approximately 350 MPa after 50% rolling reduction.

Acknowledgement We acknowledge the Danish National Research Foundation for supporting the Center for Fundamental Research: Metal Structures in Four Dimensions, within which this work was performed.

References

1. Hughes DA, Hansen N (2000) Acta Mater 48:2985
2. Liu Q, Huang X, Lloyd DJ, Hansen N (2002) Acta Mater 53:3789
3. Mishin OV, Juul Jensen D, Hansen N (2003) Mater Sci Eng A 342:320
4. Cabibbo M, Blum W, Evangelista E, Kassner ME, Meyers MA (2007) Metall Mater Trans A 39A:181
5. Wu XL, Ma E (2006) Appl Phys Lett 88:231911
6. Zhao YH, Zhu YT, Liao XZ, Horita Z, Langdon TG (2006) Appl Phys Lett 89:121906
7. Zhao YH, Bingert JF, Liao XZ, Cui BZ, Sergueeva AV, Mukherjee AK, Valiev RZ, Langdon TG, Zhu YT (2006) Adv Mater 18:2949
8. Huang X (2007) J Mater Sci 42:1577. doi:10.1007/s10853-006-0988-5
9. Zhao YH, Bingert JF, Zhu YT, Liao XZ, Valiev RZ, Horita Z, Langdon TG, Zhou YZ, Lavernia EJ (2008) Appl Phys Lett 92:081903
10. Hansen N (2004) Scr Mater 51:801
11. Hansen N, Huang X, Hughes DA (2001) Mater Sci Eng A 317:3
12. Huang X, Kamikawa N, Hansen N (2008) Mater Sci Eng. doi:10.1016/j.msea.2007.04.131
13. Ma E (2003) Scr Mater 49:663
14. Huang X, Hansen N, Tsuji N (2006) Science 312:249
15. Huang X, Kamikawa N, Hansen N (2008) Mater Sci Eng 483–484:102
16. Kamikawa N, Sakai T, Tsuji N (2007) Acta Mater 55:5873
17. Winther G, Huang X, Godfrey A, Hansen N (2004) Acta Mater 52:4437
18. Liu Q (1995) Ultramicroscopy 60:81